TU Delft

Delft University of Technology

Mesozoic and Cenozoic thermal history of the Western Reguibat Shield (West African Craton)

Gouiza, Mohamed; Bertotti, Giovanni; Andriessen, Paul A.M.

DOI
10.1111/ter.12318

Publication date
2018

Document Version
Final published version

Published in
Terra Nova: the European journal of geosciences

Citation (APA)
Gouiza, M., Bertotti, G., & Andriessen, P. A. M. (2018). Mesozoic and Cenozoic thermal history of the Western Reguibat Shield (West African Craton). *Terra Nova: the European journal of geosciences*, *30*(2), 135-145. https://doi.org/10.1111/ter.12318

Important note
To cite this publication, please use the final published version (if applicable).
Please check the document version above.

Copyright
Other than for strictly personal use, it is not permitted to download, forward or distribute the text or part of it, without the consent of the author(s) and/or copyright holder(s), unless the work is under an open content license such as Creative Commons.

Takedown policy
Please contact us and provide details if you believe this document breaches copyrights.
We will remove access to the work immediately and investigate your claim.

This work is downloaded from Delft University of Technology.
For technical reasons the number of authors shown on this cover page is limited to a maximum of 10.

Received: 19 December 2016 | Revised: 8 November 2017 | Accepted: 20 November 2017

DOI: 10.1111/ter.12318

PAPER

WILEY Terra Nova

Mesozoic and Cenozoic thermal history of the Western Reguibat Shield (West African Craton)

Mohamed Gouiza[1] | Giovanni Bertotti[2] | Paul A. M. Andriessen[3]

[1]School of Earth and Environment, University of Leeds, Leeds, UK

[2]Faculty of Civil Engineering and Geosciences, TU Delft, Delft, The Netherlands

[3]Faculty of Earth Sciences, VU University Amsterdam, Amsterdam, The Netherlands

Correspondence
Mohamed Gouiza, School of Earth and Environment, University of Leeds, Leeds, UK.
Email: m.gouiza@leeds.ac.uk

Abstract

Using low-temperature thermochronology on apatite and zircon crystals, we show that the western Reguibat Shield, located in the northern part of the West African Craton, experienced significant cooling and heating events between Jurassic and present times. The obtained apatite fission track ages range between 49 and 102 Ma with mean track lengths varying between 11.6 and 13.3 μm and Dpar values between 1.69 and 3.08 μm. Zircon fission track analysis yielded two ages of 159 and 118 Ma. Apatite (U–Th)/He uncorrected single-grain ages range between 76 and 95 Ma. Thermal inverse modelling indicates that the Reguibat Shield was exhumed during the Early Cretaceous, Late Cretaceous, Palaeocene–Eocene and Quaternary. These exhumation events were coeval with regional tectonic and geodynamic events, and were probably driven by a combined effect of plate tectonics and mantle dynamics.

1 | INTRODUCTION

A substantial number of studies examining the thermal evolution of domains contiguous to the Moroccan Atlantic margin reveal the existence of major thermal events that occurred after the Early-Middle Jurassic initiation of drifting in the Central Atlantic (e.g. Ghorbal, 2009; Ghorbal, Bertotti, Foeken, & Andriessen, 2008; Leprêtre, Barbarand, Missenard, Leparmentier, & Frizon de Lamotte, 2014; Leprêtre et al., 2015; Oukassou et al., 2013; Ruiz et al., 2011; Saddiqi et al., 2009; Sebti et al., 2009; Sehrt, 2014). These thermal events, constrained by low-temperature thermochronology (LTT) (i.e. fission track and U–Th/He analyses on apatite and zircon crystals), are systematically attributed to km-scale vertical movements of the continental crust (i.e. burial and exhumation). The supposedly exhumed domains are characterized by exposed old pre-Mesozoic basement, and the absence of sedimentary cover prevents the understanding and quantification of the tectonic processes that might have driven such evolution (Gouiza, 2011; Teixell, Bertotti, Frizon de Lamotte, & Charroud, 2009).

The Reguibat shield is a domain that experienced at least one major cooling event during Mesozoic times (Leprêtre et al., 2014, 2015). It is located in the northern part of the West African Craton and extends over 1,400 km from the Algerian Sahara domain in the east to the Moroccan Atlantic margin in the west (Figure 1). It is an ENE–WSW basement rise where Archaean and Palaeoproterozoic rocks are exposed (Figure 1) (Schofield et al., 2012; Villeneuve & Cornée, 1994). It is surrounded by the Variscan Mauritanides Belt in the SW (ca. 300 Ma; Lécorché, Roussel, Sougy, & Guetat, 1983; Purdy, 1987), the coastal Atlantic basin of Tarfaya in the NW, the Palaeozoic Tindouf Basin in the N–NE, and the Neoproterozoic–Palaeozoic Hank and Adrar Basins in the south (Villeneuve, 2005).

Whereas the fold belts surrounding the West African Craton (Figure 1) were folded and metamorphosed during the Pan-African and/or Variscan orogenies (e.g. Black et al., 1979; Gasquet, Ennih, Liégeois, Soulaimani, & Michard, 2008; Guiraud, Bellion, Benkhelil, & Moreau, 1987; Hoepffner, Soulaimani, & Piqué, 2005; Purdy, 1987; Soulaimani & Burkhard, 2008), the cratonic basement exposed in the Reguibat and Man-Leo shields (Figure 1) is considered to have been tectonically stable since 1,700 Ma (e.g. Villeneuve & Cornée, 1994). However, recently published apatite fission track and (U–Th)/He analyses on samples from the central and western Reguibat suggest that major post-Triassic cooling/exhumation events affected the shield (Leprêtre et al., 2015, 2017).

In this contribution, we present new LTT data from 18 samples collected from the western Reguibat shield, including 17 apatite

 © 2017 John Wiley & Sons Ltd

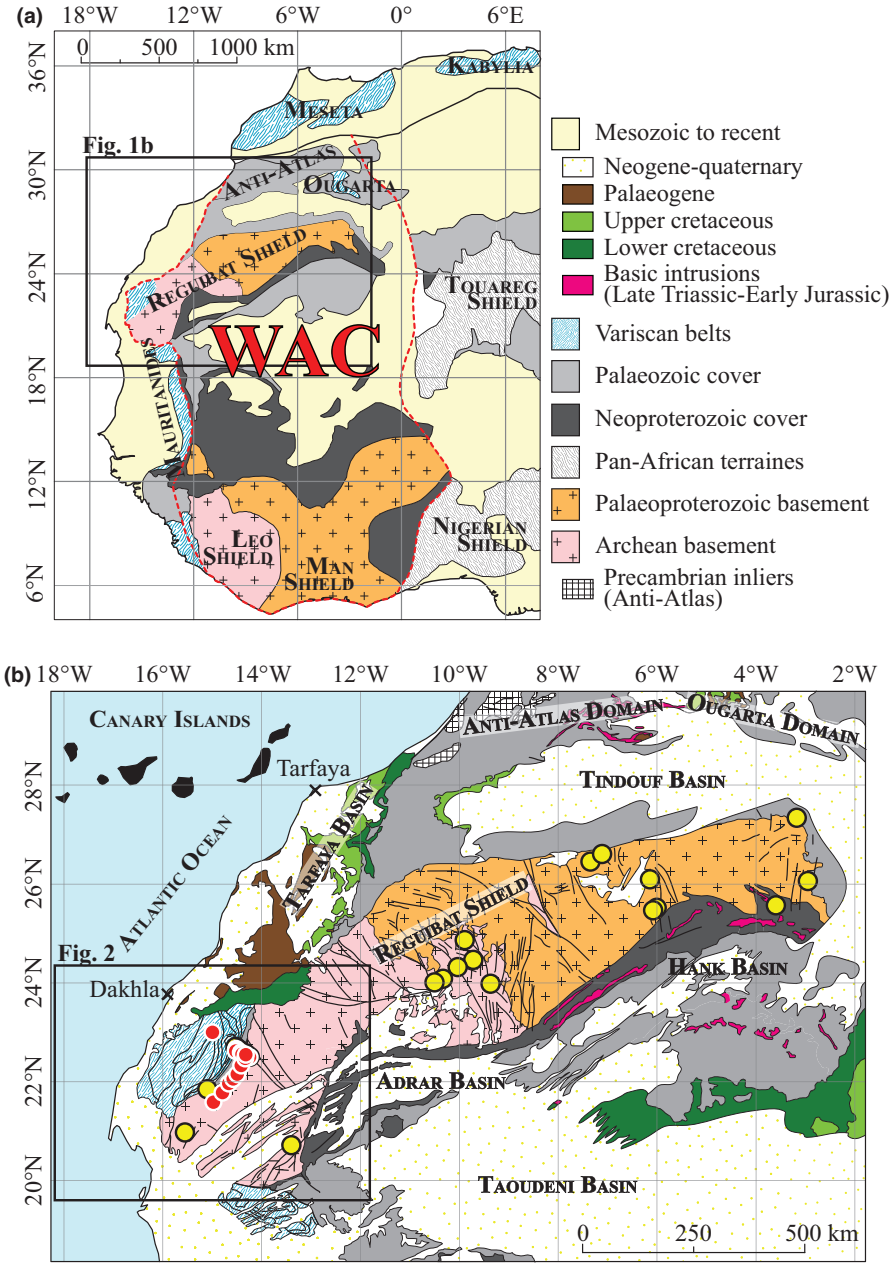

FIGURE 1 Simplified geological maps of (a) the West African Craton (WAC) and (b) the Reguibat Shield and surrounding domains (modified from the geological map of Africa 1:5,000,000 (Whiteman, 1965) and after Ennih & Liégeois, 2008). Red dots with white outlines indicate the locations of samples analysed in this study; yellow dots with black outlines indicate the locations of samples analysed by Leprêtre (2015) and Leprêtre et al. (2014, 2015)

fission track (AFT), two zircon fission track (ZFT) and seven single-grain apatite (U–Th)/He (AHe) analyses. We compare our results to previously published data (Leprêtre et al., 2014, 2015) and challenge the model of a stable craton by proposing a modified model for the tectonic and thermal evolution of the shield.

2 | METHODS AND ANALYTICAL RESULTS

Investigation of the thermal history of the western Reguibat basement rocks by AFT, ZFT and AHe analyses allows to constrain the time when the samples passed through the temperature window characteristic of each method: 350–220°C for ZFT (Yamada, Murakami, & Tagami, 2007), 110–60°C for AFT (Green et al., 1989), and 75–45°C for AHe (Farley, 2000). Fission track densities, horizontal confined track lengths and Dpar (diameter of etched spontaneous fission tracks, used as a proxy for the chemical composition of apatite) were measured in the apatite grains with internal surfaces parallel to the c-axis (Donelick, Ketcham, & Carlson, 1999).

Two batches of samples were collected from the exposed magmatic rocks intruding the Archaean basement of the western Reguibat Shield (Figure 2). The first set of samples (AW) was collected along a NW–SE transect, from the syenite, dolerite and granitoid intrusions outcropping near Awsard (Figure 2). The second set of samples (MS) was collected along a NNE–SSW transect between Awsard and Tichla (Figure 2) within the Precambrian granite intrusions. Apart from the syenite intrusions of Awsard, which are dated to be ca. 2.46 Ga (Bea, Montero, Haissen, & El, 2013), the sampled

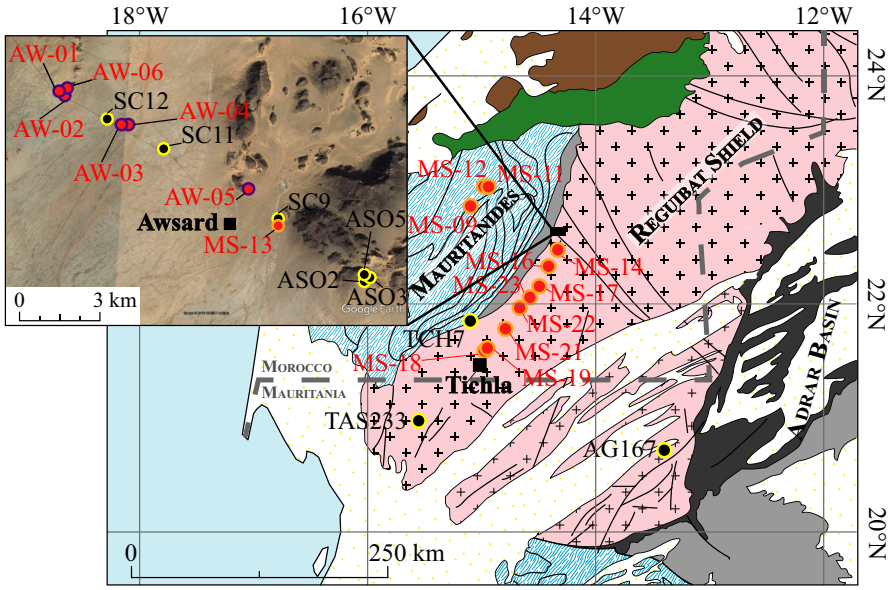

FIGURE 2 Zoom-in on the western Reguibat Shield showing in detail the locations of samples analysed in this study (red dots) and by Leprêtre et al. (2015) (black dots). MS samples are marked with orange outlines, AW samples with purple outlines. Same legend for geological units as in Figure 1

intrusions are not yet dated but are assumed to be Late Archaean to Early Palaeoproterozoic (ca. 2.9–1.8 Ga; e.g. Schofield et al., 2012; Jessell et al., 2015).

Age data from this study are presented in Tables 1 and 2. AFT ages range between 74 and 102 Ma for the AW samples, and between 49 and 87 Ma for the MS samples (Table 1). Mean track lengths (MTL) measured in apatite grains vary between 11.8 and 13.3 μm in the AW samples, and between 11.6 and 13.1 μm in the MS samples (Table 1). The measured Dpar values range from 1.69 to 3.08 μm in the AW samples, and from 1.72 to 2.95 μm in the MS samples (Table 1). ZFT analysis was performed on samples MS-09 and MS-12 and yielded ages of 159 and 118 Ma, respectively (Table 1).

AHe analysis, performed on samples AW-03, AW-05 and AW-06, yielded uncorrected single-grain ages ranging between 76 and 95 Ma (Table 2). The α-ejection corrected single-grain ages (Farley, Wolf, & Silver, 1996) vary between 95 and 119 Ma, with single-grain ages of the same sample overlapping within 1σ uncertainty (Table 2).

We note that the AHe uncorrected ages are either younger than the AFT ages of the same sample or equal within the 1σ uncertainty level, while the AHe corrected ages are systematically older than the AFT ages of the same sample. Radiation damage in (old) apatite crystals can cause non-thermal annealing of fission tracks (e.g. Hendriks & Redfield, 2005; Söderlund, Juez-Larré, Page, & Dunai, 2005) and can increase He retentivity (e.g. Flowers, 2009; Green & Duddy, 2006; Shuster, Flowers, & Farley, 2006), which may result in an inverted relationship between AHe and AFT ages (i.e. AHe ages older than AFT ages). This is usually associated with a positive correlation between effective uranium concentration (eU) and AHe ages (Brown et al., 2013; Fitzgerald, Baldwin, Webb, & O'Sullivan, 2006), which is not the case for the Reguibat samples (Table 2). Over-correction for α-ejection, due to U and Th zonation in apatite crystals, may instead be responsible for the inverted relation between AFT ages and corrected AHe ages observed in our data (Hourigan, Reiners, & Brandon, 2005).

2.1 | Published thermochronology ages

Leprêtre (2015) and Leprêtre et al. (2014, 2015) presented AFT and AHe analyses on samples from the entire Reguibat Shield (Figure 1). According to their studies, AFT single-grain ages from the western Reguibat range from 108 to 176 Ma, while α-ejection corrected AHe ages range from 14 to 185 Ma. In the central Reguibat, AFT ages vary from 139 to 256 Ma, while α-ejection corrected AHe ages vary from 93 to 149 Ma. In the eastern Reguibat, AFT ages vary from 166 to 497 Ma, while α-ejection corrected AHe ages vary from 40 to 198 Ma. These studies show that the AFT ages get substantially younger westwards, i.e. towards the Atlantic margin.

Overall, AFT ages from Leprêtre et al. (2015) from the Western Reguibat are distinctly older than the AFT ages obtained in this study. Even contiguous granitic samples such as SC9 and MS-13, which were sampled only 300 m apart, and are thus expected to belong to the same intrusive body, produce AFT ages of 143 ± 13 Ma and 57.8 ± 2.7 Ma, respectively. Single-grain AFT data from Leprêtre et al. (2015) reveal a significant spread in individual grain ages, which could be related to variations in apatite chemistry (i.e. chlorine-rich vs. fluorine-rich apatites; see O'Sullivan & Parrish, 1995; Barbarand, Carter, Wood, & Hurford, 2003).

2.2 | Thermal modelling

We used QTQt software (Gallagher, 2012) to model the thermal history of the western Reguibat Shield. QTQt is based on the Bayesian transdimensional Markov Chain Monte Carlo method (Denison, Holmes, Mallick, & Smith, 2002; Gilks, Richardson, & Spiegelhalter, 1995) and allows the sampling of a wide range of thermal histories

TABLE 1 Analytical results of apatite fission track analyses of the samples collected from the Moroccan Reguibat Shield. Errors are ± 1σ, calculated using the Zeta calibration technique (ζAFT = 335 ± 22 for AW samples; ζAFT = 358 ± 10 and ζZFT = 128 ± 3 for MS samples). ρ_s and ρ_i are the spontaneous and induced track densities, respectively; N_s and N_i are the numbers of spontaneous and induced tracks, respectively. For samples passing the $P(\chi^2)$ >5%, pooled ages were calculated. For AW-02 ($P(\chi^2)$ = 2.42%) a central age was calculated. ρ_d = 0.80532x10^6 tr/cm^2 (N_d = 16627) for AW samples. For MS samples: ρ_d =1.0537 × 10^6 tr/cm^2 (N_d = 21755) for AFT and ρ_d = 0.47194 × 10^6 tr/cm^2 (N_d = 9744) for ZFT

Sample	Coordinates	Elevation (m)	Rock type	Mineral	Number of grains	ρ_s 10^6 tr/cm^2 (N_s)	ρ_i 10^6 tr/cm^2 (N_i)	$P(\chi^2)$ (%)	Fission track age (Ma)	Mean track length (μm) (# measured lengths)	Min–max Dpar (μm) (# measured Dpar)
AW-01	N22°35′46.05″ W14°24′04.40″	302	Granitoid	Apatite	21	1.2728 (1630)	2.0287 (2598)	44.94	83.8 ± 6.2	11.77 ± 0.19 (101)	1.76–2.30 (21)
AW-02	N22°35′50.09″ W14°24′01.21″	310	Syenite	Apatite	17	1.1599 (1893)	2.0711 (3380)	2.42	74.0 ± 5.8	12.71 ± 0.15 (101)	1.69–2.26 (17)
AW-03	N22°35′01.15″ W14°22′28.41″	290	Doleritic dyke	Apatite	20	0.7107 (1340)	1.1016 (2077)	91.21	86.2 ± 6.5	11.76 ± 0.24 (59)	1.782–2.255 (20)
AW-04	N22°35′01.57″ W14°22′36.38″	290	Doleritic dyke	Apatite	9	1.1753 (510)	1.6339 (709)	91.62	95.4 ± 8.4	13.29 ± 0.47 (18)	1.81–3.03 (8)
AW-05	N22°33′41.75″ W14°19′31.38″	320	Syenite	Apatite	12	1.9688 (2268)	3.0451 (3508)	95.93	86.4 ± 6.2	12.71 ± 0.15 (111)	1.88–2.32 (12)
AW-06	N22°35′47.39″ W14°24′03.18″	315	Syenite	Apatite	15	1.9419 (2692)	2.5472 (3531)	54.77	101.7 ± 7.2	12.80 ± 0.12 (120)	1.87–2.31 (15)
MS-09	N22°51′45.71″ W15°05′50.82″	191	Granite	Zircon	10	9.599 (1115)	1.799 (209)	100	159.2 ± 12.7	-	-
MS-11	N23°01′6.74″ W15°00′04.15″	222	Granite	Apatite	15	0.0889 (124)	0.2522 (352)	100	66.1 ± 7.2	12.30 ± 0.33 (8)	1.79–2.35 (75)
MS-12	N23°01′9.32″ W15°00′14.45″	218	Granite	Apatite	11	1.9425 (2094)	4.1837 (4510)	98.9	87.0 ± 3.4	12.37 ± 0.1 (210)	1.82–2.19 (56)
				Zircon	9	10.341 (1241)	2.633 (316)	92.7	117.5 ± 8.0	-	-
MS-13	N22°32′57.96″ W14°18′53.40″	310	Granite	Apatite	12	0.9524 (967)	3.0957 (3143)	98.1	57.8 ± 2.7	12.29 ± 0.16 (102)	1.86–2.79 (60)
MS-14	N22°29′44.27″ W14°19′47.95″	277	Granite	Apatite	15	0.2586 (370)	0.9841 (1408)	99.9	49.4 ± 3.2	13.13 ± 0.14 (96)	1.96–2.66 (75)
MS-16	N22°22′44.24″ W14°32′03.27″	271	Granite	Apatite	10	0.6745 (661)	2.5765 (2525)	95.4	49.2 ± 2.6	12.75 ± 0.14 (108)	1.85–2.46 (51)
MS-17	N22°11′38.69″ W14°28′57.23″	266	Granite	Apatite	10	0.8455 (696)	2.4514 (2018)	94	64.7 ± 3.4	12.39 ± 0.15 (90)	1.72–2.95 (50)
MS-18	N22°05′01.88″ W14°34′38.63″	176	Granite	Apatite	15	0.2259 (321)	0.7241 (1029)	100	58.6 ± 4.1	12.15 ± 0.27 (38)	1.74–2.14 (75)
MS-19	N22°00′31.50″ W14°39′05.23″	177	Granite	Apatite	15	0.2986 (439)	0.9762 (1435)	100	57.4 ± 3.4	12.22 ± 0.23 (61)	1.69–2.28 (75)
MS-21	N21°47′35.28″ W14°48′03.66″	212	Granite	Apatite	19	0.2684 (483)	1.1116 (2000)	100	45.4 ± 2.6	11.63 ± 0.18 (100)	1.92–2.28 (90)
MS-22	N21°36′04.96″ W14°57′42.34″	245	Granite	Apatite	15	0.878 (1206)	2.5924 (3567)	99.6	63.6 ± 2.8	12.11 ± 0.19 (112)	1.75–2.29 (75)
MS-23	N21°35′57.63″ W14°57′52.82″	240	Granite	Apatite	15	0.6279 (923)	1.7925 (2635)	93.8	65.7 ± 3.1	12.12 ± 0.16 (102)	1.77–2.10 (77)

TABLE 2 Analytical results of apatite (U–Th)/He analyses of AW samples. Uncorrected and α-ejection corrected ages (=uncorrected age/Ft) are shown. Errors are calculated by adding errors from the analytical procedure, the crystal size and the variability of the measured Durango standard. α-ejection correction is calculated to account for alpha loss in the outer 20 μm of the apatite crystal (Farley et al., 1996)

Sample	Coordinates	Crystal length (μm)	Crystal radius (μm)	Mass (μg)	^{4}He (ncc/gm)	^{238}U (ppm)	^{232}Th (ppm)	Th/U	eU (ppm)	Uncorrected AHe age (Ma)	Error	Ft factor	Corrected AHe age (Ma)	Error
AW-03-I	N22°35′0.24″	247	76	7.60	1.25E+05	6.71	17.15	2.55	10.74	94.6	8.9	0.80	118.8	11.2
AW-03-III	W14°22′33.52″	250	76	8.61	1.38E+05	10.13	20.26	2.00	14.90	75.5	7.5	0.80	94.5	9.3
AW-05-I	N22°33′41.86″	215	62	8.04	3.06E+05	31.01	5.06	0.16	32.20	80.1	7.5	0.77	103.8	9.8
AW-05-III	W14°19′36.51″	234	64	7.42	8.07E+05	71.19	19.09	0.27	75.67	87.0	8.2	0.78	111.7	10.5
AW-06-I	N22°35′47.42″	328	86	15.76	8.75E+04	7.97	1.91	0.24	8.42	84.9	8.4	0.84	101.6	10.1
AW-06-II	W14°24′4.83″	237	86	29.51	6.48E+05	61.47	13.86	0.23	64.73	81.7	8.1	0.82	99.1	9.8
AW-06-III		193	80	7.78	6.64E+05	53.74	13.50	0.25	56.91	95.1	9.0	0.81	118.0	11.1
Dur11	-	-	-	-	2.67E+05	11.37	216.93	19.08	62.35	35.1	3.3	-	-	-
Dur12	-	-	-	-	2.62E+05	9.37	217.62	23.22	60.51	35.5	3.3	-	-	-

constrained by fission track and (U–Th)/He data. The output of the modelling is a collection of time–temperature (t–T) scenarios and other specific t–T paths, such as the maximum likelihood model (i.e. best data-fitting model) and the expected model (i.e. a weighted mean model from the probability distribution of the sampled t–T paths). The fit between the observed and predicted data is defined by a likelihood function, which quantifies the probability of obtaining the data given by the model. The higher the likelihood log value the better the model fits the data. In addition, the validity of a model must be checked by examining the stability of the log likelihood and the number of t–T points at each iteration. More details about the modelling method are given in Gallagher (2012).

Given the narrow spatial distribution of the samples and the lack of Meso-Cenozoic tectonic structures in the sampled area that could cause varying thermal histories among the samples, we believe that the LTT data illustrate a uniform thermal history and that variations in FT ages are related to compositional changes among the dated apatites (Barbarand et al., 2003; O'Sullivan & Parrish, 1995). Thus, for the purpose of thermal modelling, we combined the AFT data from the six AW samples (Figure 3a), the AFT data from the eleven MS samples (Figure 3b) and the ZFT data from MS-09 to MS-12 (Figure 3c). Due to the range of the LTT ages, we only model the thermal evolution during post-Triassic times (i.e. between 200 and 0 Ma). Initial inverse modelling was carried out to explore several modelling configurations and the modelling sensitivity to He kinetics (Flowers, 2009; Gautheron, Tassan-Got, Barbarand, & Pagel, 2009) and ZFT annealing models (Tagami, Lal, Sorkhabi, Ito, & Nishimura, 1988; Yamada et al., 2007). These initial models are presented in the Supplementary Data S1. The final QTQt simulation (Figure 4) uses the He kinetics of Flowers (2009) and the annealing models of Ketcham, Carter, Donelick, Barbarand, and Hurford (2007) and Yamada et al. (2007) for apatite and zircon, respectively. Our test models indicate that changing the ZFT annealing model and the He kinetics have a limited impact on the predicted t–T history (Figures S4, S5, S6, S8 and S9); however, the He kinetics of Flowers (2009) (Figs. S4, S5 and S6) and the ZFT annealing model of Yamada et al. (2007) (Figures S8 and S9) best correspond to the observed AHe and ZFT ages, respectively.

The obtained maximum likelihood t–T path (Figure 4) is characterized by a major rapid cooling event (−370°C) during the Early Cretaceous (between 130 and 120 Ma) followed by a thermally unstable period (between 120 and 0 Ma) with potentially three additional cooling events of lesser magnitudes at 80–70 Ma (−50°C), 60–50 Ma (−80°C) and during the Quaternary (−40°C). The predicted ZFT and AFT ages, along with the predicted track length distributions, are consistent with the observed ones (Figures 4b, c). However, the predicted uncorrected AHe ages are 30–60 Ma younger than the observed ones (Figure 4c). The thermal trend illustrated in this model is fairly similar to the one obtained by Leprêtre et al. (2015) for their samples from the western Reguibat Shield, which predicts three thermal cooling events between the Cretaceous and the present-day (i.e. 130–120 Ma [−120°C], 90–60 Ma [−30°C] and 10–0 Ma [−50°C]).

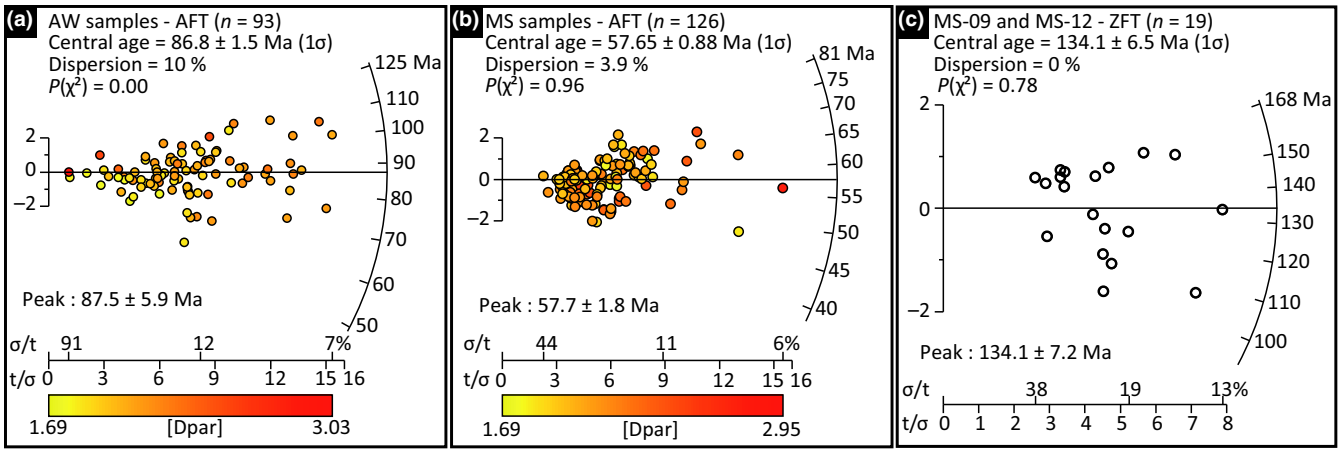

FIGURE 3 Radial plots of single grain AFT ages from (a) AW samples and (b) MS samples, and single grain ZFT ages from (c) MS-09 and MS-12

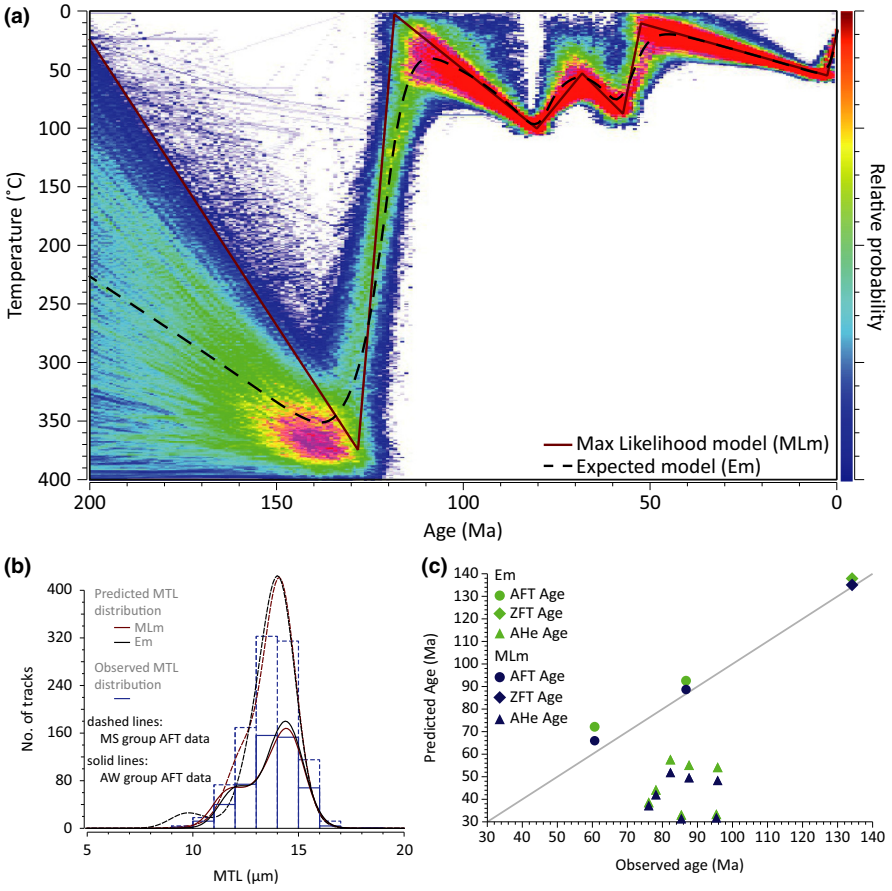

FIGURE 4 Thermal inverse modelling results constrained by ZFT, AFT and AHe data from the combined AW and MS samples. (a) Maximum Likelihood and expected t–T paths, and probability distribution of sampled thermal histories. (b) Observed and predicted apatite mean track length distributions. (c) Observed and predicted ZFT, AFT and AHe ages

2.3 | Post-Triassic evolution of the western Reguibat Shield

LTT data indicate that the western Reguibat Shield shows a differentiated post-Triassic thermal history. Inverse modelling (Figure 4) suggests a major cooling event during the Early Cretaceous, which brought the sampled basement rocks from mid-crustal to near-surface temperatures, followed by three minor heating events between the Late Cretaceous and the present-day. Heating events occurred during the Aptian–Santonian (120–80 Ma), the Maastrichtian–Early Palaeocene (70–60 Ma) and the Eocene–Pliocene (50–3 Ma).

Major magmatic events are recorded in the region, including the Late Triassic–Early Jurassic tholeiitic basalt flows and dikes of the Central Atlantic Magmatic Province (Knight et al., 2004; Marzoli et al., 2004) and the Meso-Cenozoic peri-Atlantic alkaline pulses (Matton & Jébrak, 2009). Although volcanic rocks and/or magmatic intrusions related to these magmatic events are yet to be documented in the Reguibat Shield per se, their widespread occurrence

along the margins of the Central Atlantic suggests deep mantle or at least asthenospheric origin (Matton & Jébrak, 2009). In addition, the Late Triassic–Early Jurassic rifting in the Central Atlantic involved major thermal perturbations due to the related lithospheric thinning. Increasing surface heat flux from 40 mWm^{-2} (characteristic of cratonic domains) to 90 mWm^{-2} (characteristic of rifted domains) can raise the 60°C isotherm (the upper limit of the AFT partial annealing zone) from a depth of ~5 km to ~2 km (Ehlers, 2005). However, seismic data offshore the Dakhla margin indicate that our samples are located 400 to 500 km east of the margin hinge line and that the crust underneath the western Reguibat Shield is at least 27–30 km thick (Labails & Olivet, 2009).

In domains where the crust keeps its integrity through time, large changes in surface heat flow may be accounted for only by a change in crustal heat generation, while variations in basal heat flow from the mantle have a minor impact on the upper portion of the crust (Mareschal & Jaupart, 2004). Thus, the succession of heating and cooling events documented in the western Reguibat Shield by LTT analyses is expected to be largely due to vertical movements of the crust expressed by burial/subsidence and exhumation/erosion, respectively. Given the magnitude of the modelled vertical movements/thermal events, they must be documented in the sedimentary record of the nearby basins of the Atlantic margin. Published data from the Dakhla margin (Labails & Olivet, 2009), bordering the western Reguibat Shield, do not properly illustrate the stratigraphic architecture of the margin. Well and seismic data from the Tarfaya basin, located on the NW margin of the shield, however, show several regressive events (Figure 5; El Jorfi, Süss, Aigner, & Mhammdi, 2015), certainly associated with, or even driven by, the exhumation of the hinterlands and their erosion. Thus, the Hauterivian–Aptian (130–120 Ma) and the Campanian (80–70 Ma) cooling events correlate with decreases in relative sea level and erosional unconformities in the Tarfaya continental shelf (Figure 5). The Middle–Late Palaeocene (60–50 Ma) cooling event appears to coincide with the end of a transgressive phase according to El Jorfi et al. (2015), which persisted through the Eocene and Early Oligocene (Figure 5; El Jorfi et al., 2015; Gouiza, 2011).

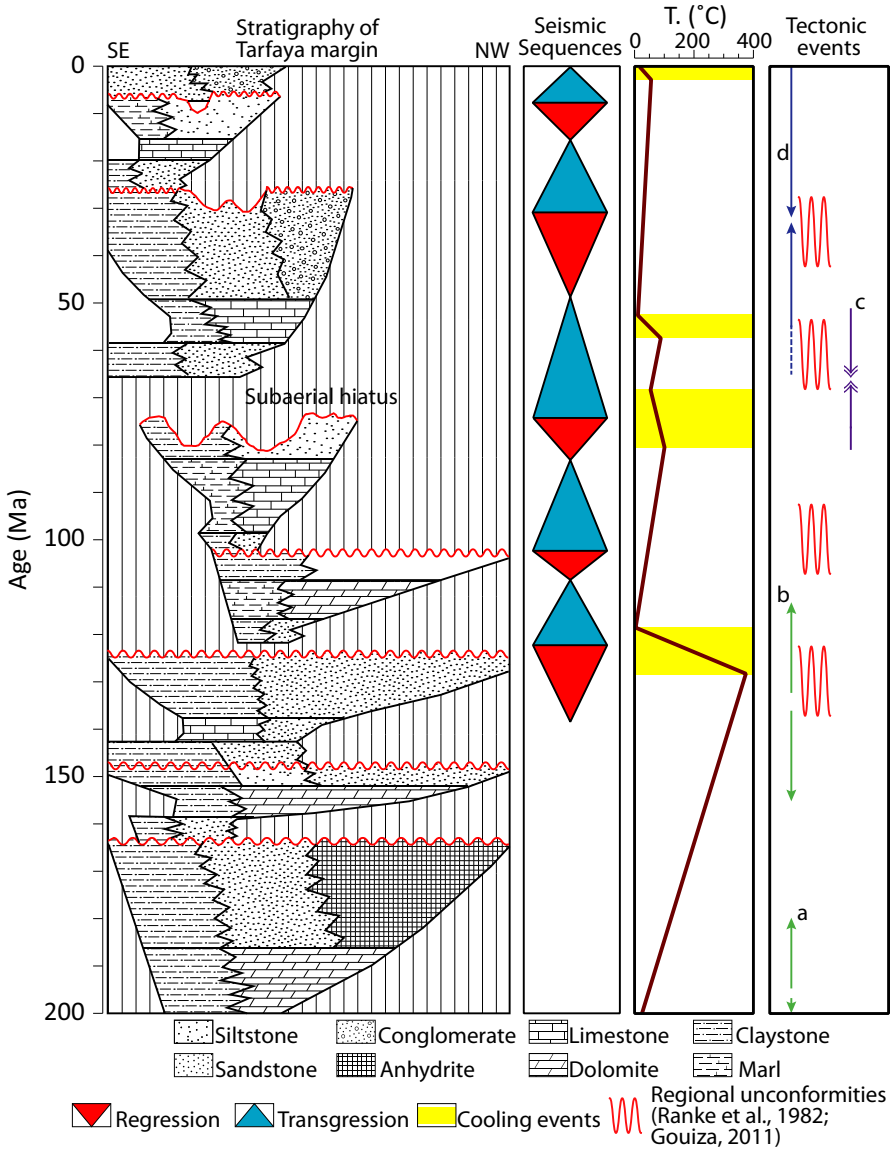

FIGURE 5 Chronostratigraphic chart of the Tarfaya basin showing the sedimentary gaps and seismic sequences (El Jorfi et al., 2015) with respect to the maximum likelihood t–T path obtained from the thermal modelling and the regional tectonic events [a: Central Atlantic Rift (Klitgord, Schouten, Vogt, & Tucholke, 1986); b: South Atlantic Rift (Torsvik, Rousse, Labails, & Smethurst, 2009); c: Africa–Iberia collision (Martínez-Loriente et al., 2014); d: Rif–Atlas orogeny (Frizon De Lamotte, Andrieux, & Guezou, 1991; Piqué et al., 2002)]

The major cooling event recorded during the Hauterivian–Aptian, which brought the basement rocks from mid-crust to near-surface temperatures, is consistent with low-temperature thermochronology results from the Anti-Atlas domain in the north (Gouiza, Charton, Bertotti, Andriessen, & Storms, 2017; Oukassou et al., 2013; Ruiz et al., 2011). It is also coherent with the presence of Lower Cretaceous sediments unconformably lying on the fringe of the Reguibat basement in the north (Figure 1), although these sediments have yet to be properly dated.

The heating events on the other hand are attributed to subsidence and basement burial, which means that Mesozoic sediments were deposited on the western Reguibat Shield and later eroded during the following exhumation phases. The eroded sediments were probably routed to the Atlantic shelf and deep basin (Davison, 2005; Gouiza, 2011).

The geological processes driving these thermal events/km-scale vertical movements are unclear, especially since similar vertical movements are documented all along the Moroccan margin (e.g. Ghorbal et al., 2008; Gouiza et al., 2017; Malusà et al., 2007; Oukassou et al., 2013; Ruiz et al., 2011) and the East American conjugate as well (e.g. Grist & Zentilli, 2003; Roden-Tice & Tice, 2005; Roden-Tice & Wintsch, 2002). Bertotti & Gouiza (2012) proposed that the Late Jurassic–Early Cretaceous exhumation recorded in the Meseta and the High Atlas (Figure 1) is related to coeval regional shortening, documented by syn-sedimentary tectonics in the Essaouira basin, which is located in the western High Atlas to the south of the Meseta. Leprêtre et al. (2017), on the other hand, proposed transient mantle dynamics to account for the major erosional phases recorded on both sides of the Atlantic. Gouiza (2011) investigated the effect of small-scale sublithospheric mantle convection on crustal exhumation, using thermo-mechanical numerical modelling, and showed that the surface response to mantle dynamics underneath continental lithosphere is limited to a few hundreds of metres. However, the numerical modelling did not incorporate erosion, which is known to enhance crustal exhumation.

We hypothesise that the major Early Cretaceous exhumation/cooling was driven by the combined action of regional compressional stresses and sublithospheric mantle dynamics. The regional stresses are related to the readjustment of the African plate to the differential opening of the Central, South and North Atlantics, while mantle dynamics are inherited from the rift system and triggered by the established lateral thermal gradient between thinned and unthinned continental lithosphere (Buck, 1986).

The following cooling events, during the Late Cretaceous, the Palaeocene and the Quaternary, occurred during Africa–Europe convergence, which began during the Senonian (e.g. Ricou, 1994). Frizon De Lamotte et al. (2009) argued that this convergence was accommodated through time by large wavelength folding/buckling of the African lithosphere during the Late Cretaceous and Palaeocene, and by inversion of the intracontinental rifts (e.g. Atlas rifts) typically during the Middle–Late Eocene and the Pliocene–Quaternary.

3 | CONCLUSION

The LTT data indicate that the basement of the western Reguibat Shield experienced a succession of cooling and heating events during Mesozoic and Cenozoic times. According to inverse thermal modelling, a major cooling episode occurred during the Early Cretaceous (130–120 Ma), followed by minor cooling episodes during the Campanian (80–70 Ma), the Middle–Late Palaeocene (60–50 Ma) and the Quaternary (3–0 Ma). These cooling phases are interpreted to be episodes of crustal exhumation, while the heating events are interpreted to reflect subsidence and burial. The exhumation episodes correlate with regressive events and erosional unconformities documented in well and seismic data from the neighbouring Atlantic basin of Tarfaya.

Since similar exhumation events are recorded in other domains of the Atlantic margin, in Morocco and in eastern North America, we believe that they are driven by regional processes. The processes are thought to involve the combined action of regional compressional stresses and subcontinental mantle dynamics. The regional stresses are related to plate tectonics and the readjustment of the African plate to the differential opening of the Central, South and North Atlantics, while the mantle dynamics are due to lateral thermal gradients between thinned and unthinned continental lithosphere established during the Atlantic rifting.

ACKNOWLEDGEMENTS

We are very grateful to the Associate Editor M. Rahn, Prof. J.-P. Liégeois, Prof. D. Frizon de Lamotte, and an anonymous reviewer for their excellent reviews of our manuscript, which helped improve its quality.

ORCID

Mohamed Gouiza http://orcid.org/0000-0001-5438-2698

REFERENCES

Barbarand, J., Carter, A., Wood, I., & Hurford, T. (2003). Compositional and structural control of fission-track annealing in apatite. *Chemical Geology*, *198*, 107–137. https://doi.org/10.1016/S0009-2541(02)00424-2

Bea, F., Montero, P., Haissen, F., & El, A. (2013). 2.46 Ga kalsilite and nepheline syenites from the Awsard pluton, Reguibat Rise of the West African Craton, Morocco. *Generation of extremely K-rich magmas at the Archean-Proterozoic transition: Precambrian Research*, *224*, 242–254. https://doi.org/10.1016/j.precamres.2012.09.024

Bertotti, G., & Gouiza, M. (2012). Post-rift vertical movements and horizontal deformations in the eastern margin of the Central Atlantic: Middle Jurassic to Early Cretaceous evolution of Morocco. *International Journal of Earth Sciences*, *101*, 2151–2165. https://doi.org/10.1007/s00531-012-0773-4

Black, R., Caby, R., Moussine-Pouchkine, A., Bayer, R., Bertrand, J. M., Boullier, A. M., … Lesquer, A. (1979). Evidence for late Precambrian

plate tectonics in West Africa. *Nature*, *278*, 223–227. https://doi.org/10.1038/278223a0

Brown, R. W., Beucher, R., Roper, S., Persano, C., Stuart, F., & Fitzgerald, P. (2013). Natural age dispersion arising from the analysis of broken crystals. Part I: Theoretical basis and implications for the apatite (U–Th)/He thermochronometer. *Geochimica et Cosmochimica Acta*, *122*, 478–497. https://doi.org/10.1016/j.gca.2013.05.041

Buck, W. R. (1986). Small-scale convection induced by passive rifting: The cause for uplift of rift shoulders. *Earth and Planetary Science Letters*, *77*, 362–372. https://doi.org/10.1016/0012-821X(86)90146-9

Davison, I. (2005). Central Atlantic margin basins of North West Africa: Geology and hydrocarbon potential (Morocco to Guinea). *Journal of African Earth Sciences*, *43*, 254–274. https://doi.org/10.1016/j.jafrearsci.2005.07.018

Denison, T. D. G., Holmes, C. C., Mallick, B. K., & Smith, A. F. M. (2002). *Bayesian Methods for Nonlinear Classification and Regression: Wiley*. Chichester: U. K.

Donelick, R. A., Ketcham, R. A., & Carlson, W. D. (1999). Variability of apatite fission-track annealing kinetics: II. *Crystallographic orientation effects: American Mineralogist*, *84*, 1224–1234.

Ehlers, T. A. (2005). Crustal thermal processes and the interpretation of thermochronometer data. *Reviews in Mineralogy and Geochemistry*, *58*, 315–350. https://doi.org/10.2138/rmg.2005.58.12

El Jorfi, L., Süss, M. P., Aigner, T., & Mhammdi, N. (2015). Triassic – Quaternary Sequence Stratigraphy of the Tarfaya Basin (moroccan Atlantic): Structural Evolution. *Eustasy and Sedimentation: Journal of Petroleum Geology*, *38*, 77–98. https://doi.org/10.1111/jpg.12599

Ennih, N., & Liégeois, J.-P. (2008). The boundaries of the West African craton, with special reference to the basement of the Moroccan metacratonic Anti-Atlas belt: *Geological Society*. *London*, *Special Publications*, *297*, 1–17. https://doi.org/10.1144/SP297.1

Farley, K. A. (2000). Helium diffusion from apatite: General behavior as illustrated by Durango fluorapatite: *Journal of Geophysical Research: Solid*. *Earth*, *105*, 2903–2914. https://doi.org/10.1029/1999JB900348

Farley, K. A., Wolf, R. A., & Silver, L. T. (1996). The effects of long alpha-stopping distances on (U-Th)/He ages. *Geochimica et Cosmochimica Acta*, *60*, 4223–4229. https://doi.org/10.1016/S0016-7037(96)00193-7

Fitzgerald, P. G., Baldwin, S. L., Webb, L. E., & O'Sullivan, P. B. (2006). Interpretation of (U–Th)/He single grain ages from slowly cooled crustal terranes: A case study from the Transantarctic Mountains of southern Victoria Land. *Chemical Geology*, *225*, 91–120. https://doi.org/10.1016/j.chemgeo.2005.09.001

Flowers, R. M. (2009). Exploiting radiation damage control on apatite (U-Th)/He dates in cratonic regions. *Earth and Planetary Science Letters*, *277*, 148–155. https://doi.org/10.1016/j.epsl.2008.10.005

Frizon De Lamotte, D., Leturmy, P., Missenard, Y., Khomsi, S., Ruiz, G., Saddiqi, O., … Michard, A. (2009). Mesozoic and Cenozoic vertical movements in the Atlas system (Algeria, Morocco, Tunisia): An overview. *Tectonophysics*, *475*, 9–28. https://doi.org/10.1016/j.tecto.2008.10.024

Frizon De Lamotte, D., Andrieux, J., & Guezou, J. C. (1991). Cinématique des chevauchements néogènes dans l'Arc betico-rifain; discussion sur les modèles géodynamiques. *Bulletin de la Société Géologique de France*, *162*, 611–626.

Gallagher, K. (2012). Transdimensional inverse thermal history modeling for quantitative thermochronology: *Journal of Geophysical Research: Solid*. *Earth*, *117*, B02408. https://doi.org/10.1029/2011JB008825

Gasquet, D., Ennih, N., Liégeois, J. P., Soulaimani, A., & Michard, A. (2008). The Pan-African Belt. In A. Michard, O. Saddiqi, A. Chalouan & de Frizon Lamotte D. (Eds.), *Continental Evolution: The Geology of Morocco* (pp. 33–64). Berlin, Heidelberg: Springer Berlin Heidelberg.

Gautheron, C., Tassan-Got, L., Barbarand, J., & Pagel, M. (2009). Effect of alpha-damage annealing on apatite (U–Th)/He thermochronology. *Chemical Geology*, *266*, 157–170. https://doi.org/10.1016/j.chemgeo.2009.06.001

Ghorbal, B. (2009). Mesozoic to Quaternary Thermo-Tectonic Evolution of Morocco (NW Africa). Ph.D Thesis, Vrije Universiteit, The Netherlands.

Ghorbal, B., Bertotti, G., Foeken, J., & Andriessen, P. (2008). Unexpected Jurassic to Neogene vertical movements in 'stable' parts of NW Africa revealed by low temperature geochronology. *Terra Nova*, *20*, 355–363. https://doi.org/10.1111/j.1365-3121.2008.00828.x

Gilks, W. R., Richardson, S., & Spiegelhalter, D. (1995). *Markov Chain Monte Carlo in Practice*. London, UK: Chapman and Hall.

Gouiza, M. (2011). Mesozoic Source-to-Sink Systems in NW Africa: Geology of Vertical Movements During the Birth and Growth of the Moroccan Rifted Margin. Ph.D Thesis, Vrije Universiteit Amsterdam, The Netherlands.

Gouiza, M., Charton, R., Bertotti, G., Andriessen, P., & Storms, J. E. A. (2017). Post-Variscan evolution of the Anti-Atlas belt of Morocco constrained from low-temperature geochronology. *International Journal of Earth Sciences*, *106*, 593–616. https://doi.org/10.1007/s00531-016-1325-0

Green, P. F., & Duddy, I. R. (2006). Interpretation of apatite (U–Th)/He ages and fission track ages from cratons. *Earth and Planetary Science Letters*, *244*, 541–547. https://doi.org/10.1016/j.epsl.2006.02.024

Green, P. F., Duddy, I. R., Laslett, G. M., Hegarty, K. A., Gleadow, A. J. W., & Lovering, J. F. (1989). Thermal annealing of fission tracks in apatite 4. *Quantitative modelling techniques and extension to geological timescales: Chemical Geology: Isotope Geoscience section*, *79*, 155–182. https://doi.org/10.1016/0168-9622(89)90018-3

Grist, A. M., & Zentilli, M. (2003). Post-Paleocene cooling in the southern Canadian Atlantic region: Evidence from apatite fission track models. *Canadian Journal of Earth Sciences*, *40*, 1279–1297.

Guiraud, R., Bellion, Y., Benkhelil, J., & Moreau, C. (1987). Post-Hercynian tectonics in Northern and Western Africa. *Geological Journal*, *22*, 433–466. https://doi.org/10.1002/gj.3350220628

Hendriks, B. W. H., & Redfield, T. F. (2005). Apatite fission track and (U-Th)/He data from Fennoscandia: An example of underestimation of fission track annealing in apatite. *Earth and Planetary Science Letters*, *236*, 443–458. https://doi.org/10.1016/j.epsl.2005.05.027

Hoepffner, C., Soulaimani, A., & Piqué, A. (2005). The Moroccan Hercynides. *Journal of African Earth Sciences*, *43*, 144–165. https://doi.org/16/j.jafrearsci.2005.09.002

Hourigan, J. K., Reiners, P. W., & Brandon, M. T. (2005). U-Th zonation-dependent alpha-ejection in (U-Th)/He chronometry. *Geochimica et Cosmochimica Acta*, *69*, 3349–3365. https://doi.org/10.1016/j.gca.2005.01.024

Jessell, M., Santoul, J., Baratoux, L., Youbi, N., Ernst, R. E., & Metelka, V., … Perrouty, S. (2015). An updated map of West African mafic dykes. *Journal of African Earth Sciences*, *112*, 440–450. https://doi.org/10.1016/j.jafrearsci.2015.01.007

Ketcham, R. A., Carter, A., Donelick, R. A., Barbarand, J., & Hurford, A. J. (2007). Improved modeling of fission-track annealing in apatite. *American Mineralogist*, *92*, 799–810. https://doi.org/10.2138/am.2007.2281

Klitgord, K. D., Schouten, H., Vogt, P. R., & Tucholke, B. E. (1986). Plate Kinematics of the Central Atlantic. In: P. R. Vogt & B. E. Tucholke (Eds.), *The Western North Atlantic Region: The Geology of North America* (pp. 351–378). USA: Geological Society of America.

Knight, K. B., Nomade, S., Renne, P. R., Marzoli, A., Bertrand, H., & Youbi, N. (2004). The Central Atlantic Magmatic Province at the Triassic-Jurassic boundary: Paleomagnetic and 40Ar/39Ar evidence from Morocco for brief, episodic volcanism. *Earth and Planetary Science Letters*, *228*, 143–160. https://doi.org/10.1016/j.epsl.2004.09.022

Labails, C., & Olivet, J.-L. (2009). Crustal structure of the SW Moroccan margin from wide-angle and reflection seismic data (the Dakhla experiment). *Part B - The tectonic heritage: Tectonophysics*, *468*, 83–97. https://doi.org/10.1016/j.tecto.2008.08.028

Lécorché, J. P., Roussel, J., Sougy, J., & Guetat, Z. (1983). An interpretation of the geology of the Mauritanides orogenic belt (West Africa) in the light of geophysical data: *Geological Society of America. Memoirs*, *158*, 131–148. https://doi.org/10.1130/MEM158-p131

Leprêtre, R. (2015). Evolution Phanérozoïque du Craton Ouest Africain et de ses Bordures Nord et Ouest. Ph.D Thesis, Université Paris Sud, Paris XI.

Leprêtre, R., Barbarand, J., Missenard, Y., Gautheron, C., Pinna-Jamme, R., & Saddiqi, O. (2017). Mesozoic evolution of NW Africa: Implications for the Central Atlantic Ocean dynamics. *Journal of the Geological Society*, https://doi.org/10.1144/jgs2016-100

Leprêtre, R., Barbarand, J., Missenard, Y., Leparmentier, F., & Frizon de Lamotte, D. (2014). Vertical movements along the northern border of the West African Craton: The Reguibat Shield and adjacent basins. *Geological Magazine*, *151*, 885–898. https://doi.org/10.1017/S0016756813000939

Leprêtre, R., Missenard, Y., Barbarand, J., Gautheron, C., Saddiqi, O., & Pinna-Jamme, R. (2015). Postrift history of the eastern central Atlantic passive margin: insights from the Saharan region of South Morocco. *Journal of Geophysical Research: Solid Earth*, *120*, 2014JB011549, https://doi.org/10.1002/2014JB011549

Malusà, M. G., Polino, R., Feroni, A. C., Ellero, A., Ottria, G., Baidder, L., & Musumeci, G. (2007). Post-Variscan tectonics in eastern Anti-Atlas (Morocco). *Terra Nova*, *19*, 481–489. https://doi.org/10.1111/j.1365-3121.2007.00775.x

Mareschal, J. C., & Jaupart, C. (2004). Variations of surface heat flow and lithospheric thermal structure beneath the North American craton. *Earth and Planetary Science Letters*, *223*, 65–77. https://doi.org/10.1016/j.epsl.2004.04.002

Martínez-Loriente, S., Sallarès, V., Gràcia, E., Bartolome, R., Dañobeitia, J. J., & Zitellini, N. (2014). Seismic and gravity constraints on the nature of the basement in the Africa-Eurasia plate boundary: New insights for the geodynamic evolution of the SW Iberian margin. *Journal of Geophysical Research: Solid Earth*, *119*, 2013JB010476. https://doi.org/10.1002/2013JB010476

Marzoli, A., Bertrand, H., Knight, K. B., Cirilli, S., Buratti, N., Vérati, C., … Bellieni, G. (2004). Synchrony of the Central Atlantic magmatic province and the Triassic-Jurassic boundary climatic and biotic crisis. *Geology*, *32*, 973–976. https://doi.org/10.1130/G20652.1

Matton, G., & Jébrak, M. (2009). The Cretaceous Peri-Atlantic Alkaline Pulse (PAAP): Deep mantle plume origin or shallow lithospheric break-up? *Tectonophysics*, *469*, 1–12. https://doi.org/10.1016/j.tecto.2009.01.001

O'Sullivan, P. B., & Parrish, R. R. (1995). The importance of apatite composition and single-grain ages when interpreting fission track data from plutonic rocks: A case study from the Coast Ranges. *British Columbia: Earth and Planetary Science Letters*, *132*, 213–224. https://doi.org/10.1016/0012-821X(95)00058-K

Oukassou, M., Saddiqi, O., Barbarand, J., Sebti, S., Baidder, L., & Michard, A. (2013). Post-Variscan exhumation of the Central Anti-Atlas (Morocco) constrained by zircon and apatite fission-track thermochronology. *Terra Nova*, *25*, 151–159. https://doi.org/10.1111/ter.12019

Piqué, A., Tricart, P., Guiraud, R., Laville, E., Bouaziz, S., Amrhar, M., & Ait Ouali, R. (2002). The Mesozoic-Cenozoic Atlas belt (North Africa): An overview. *Geodinamica Acta*, *15*, 185–208. https://doi.org/10.1016/S0985-3111(02)01088-4

Purdy, G. M. (1987). Regional trends in the geology of the Appalachian-Caledonian-Hercynian-Mauritanide orogen. *Earth-Science Reviews*, *24*, 279–280. https://doi.org/10.1016/0012-8252(87)90063-8

Ricou, L.-E. (1994). Tethys reconstructed: Plates, continental fragments and their Boundaries since 260 Ma from Central America to Southeastern Asia. *Geodinamica Acta*, *7*, 169–218. https://doi.org/10.1080/09853111.1994.11105266

Roden-Tice, M. K., & Tice, S. J. (2005). Regional-Scale Mid-Jurassic to Late Cretaceous Unroofing from the Adirondack Mountains through Central New England Based on Apatite Fission-Track and (U-Th)/He Thermochronology. *The Journal of Geology*, *113*, 535–552.

Roden-Tice, M. K., & Wintsch, R. P. (2002). Early Cretaceous Normal Faulting in Southern New England: Evidence from Apatite and Zircon Fission-Track Ages. *The Journal of Geology*, *110*, 159–178.

Ruiz, G. M. H., Sebti, S., Negro, F., Saddiqi, O., Frizon de Lamotte, D., Stockli, D., … Schaer, J.-P. (2011). From central Atlantic continental rift to Neogene uplift - western Anti-Atlas (Morocco). *Terra Nova*, *23*, 35–41. https://doi.org/10.1111/j.1365-3121.2010.00980.x

Saddiqi, O., El Haimer, F.-Z., Michard, A., Barbarand, J., Ruiz, G. M. H., Mansour, E. M., … Frizon de Lamotte, D. (2009). Apatite fission-track analyses on basement granites from south-western Meseta, Morocco: Paleogeographic implications and interpretation of AFT age discrepancies. *Tectonophysics*, *475*, 29–37. https://doi.org/10.1016/j.tecto.2009.01.007

Schofield, D. I., Horstwood, M. S. A., Pitfield, P. E. J., Gillespie, M., Darbyshire, F., O'Connor, E. A., & Abdouloye, T. B. (2012). U-Pb dating and Sm–Nd isotopic analysis of granitic rocks from the Tiris Complex: New constaints on key events in the evolution of the Reguibat Shield, Mauritania. *Precambrian Research*, *204–205*, 1–11. https://doi.org/10.1016/j.precamres.2011.12.008

Sebti, S., Saddiqi, O., El Haimer, F. Z., Michard, A., Ruiz, G., Bousquet, R., … Frizon de Lamotte, D. (2009). Vertical movements at the fringe of the West African Craton: First zircon fission track datings from the Anti-Atlas Precambrian basement, Morocco: *Comptes Rendus. Geosciences*, *341*, 71–77. https://doi.org/10.1016/j.crte.2008.11.006

Sehrt, M. (2014). Variscan to Neogene Long-Term Landscape Evolution at the Moroccan Passive Continental Margin (Tarfaya Basin and Western Anti-Atlas). Ph.D Thesis, Heidelberg University, Germany.

Shuster, D. L., Flowers, R. M., & Farley, K. A. (2006). The influence of natural radiation damage on helium diffusion kinetics in apatite. *Earth and Planetary Science Letters*, *249*, 148–161. https://doi.org/10.1016/j.epsl.2006.07.028

Söderlund, P., Juez-Larré, J., Page, L. M., & Dunai, T. J. (2005). Extending the time range of apatite (U-Th)/He thermochronometry in slowly cooled terranes: Palaeozoic to Cenozoic exhumation history of southeast Sweden. *Earth and Planetary Science Letters*, *239*, 266–275. https://doi.org/10.1016/j.epsl.2005.09.009

Soulaimani, A., & Burkhard, M. (2008). The Anti-Atlas chain (Morocco): The southern margin of the Variscan belt along the edge of the West African craton: *Geological Society. London, Special Publications*, *297*, 433–452. https://doi.org/10.1144/SP297.20

Tagami, T., Lal, N., Sorkhabi, R. B., Ito, H., & Nishimura, S. (1988). Fission track dating using external detector method: *Memoirs of the Faculty of Science. Kyoto University, Series of Geology and Mineralogy*, *53*, 1–30.

Teixell, A., Bertotti, G., Frizon de Lamotte, D., & Charroud, M. (2009). The geology of vertical movements of the lithosphere: An overview. *Tectonophysics*, *475*, 1–8. https://doi.org/10.1016/j.tecto.2009.08.018

Torsvik, T. H., Rousse, S., Labails, C., & Smethurst, M. A. (2009). A new scheme for the opening of the South Atlantic Ocean and the dissection of an Aptian salt basin. *Geophysical Journal International*, *177*, 1315–1333. https://doi.org/10.1111/j.1365-246X.2009.04137.x

Villeneuve, M. (2005). Paleozoic basins in West Africa and the Mauritanide thrust belt. *Journal of African Earth Sciences*, *43*, 166–195. https://doi.org/16/j.jafrearsci.2005.07.012

Villeneuve, M., & Cornée, J. J. (1994). Structure, evolution and palaeogeography of the West African craton and bordering belts during the Neoproterozoic. *Precambrian Research*, *69*, 307–326. https://doi.org/16/0301-9268(94)90094-9

Whiteman, A. J. (1965). The geological map of Africa, scale 1:5,000,000, new edition 1963. *Geological Magazine*, *102*, 80–86.
Yamada, R., Murakami, M., & Tagami, T. (2007). Statistical modelling of annealing kinetics of fission tracks in zircon. *Reassessment of laboratory experiments: Chemical Geology*, *236*, 75–91. https://doi.org/10.1016/j.chemgeo.2006.09.002

SUPPORTING INFORMATION

Additional Supporting Information may be found online in the supporting information tab for this article.

Supplementary Data S1 Initial inverse modelling, carried out to explore several modelling configurations and the thermal modelling sensitivity.

How to cite this article: Gouiza M, Bertotti G, Andriessen PAM. Mesozoic and Cenozoic thermal history of the Western Reguibat Shield (West African Craton). *Terra Nova*. 2018;30:135–145. https://doi.org/10.1111/ter.12318